Sharp Contrasts in Low-Energy Quasiparticle Dynamics of Graphite between Brillouin Zone *K* and *H* Points

J. D. Lee,[1] S. W. Han,[1] and J. Inoue[2]

[1]*School of Materials Science, Japan Advanced Institute of Science and Technology, Ishikawa 923-1292, Japan*
[2]*Quantum Dot Research Center, National Institute for Materials Science, Tsukuba 305-0044, Japan*

(Received 6 December 2007; published 29 May 2008)

The low-energy quasiparticle (QP) dynamics of graphite are governed by a coupling with the E_{2g} longitudinal optical phonon of $\omega_{\mathrm{LO}} \approx 200$ meV, which is found to dramatically depend on the electronic band dispersion $\varepsilon_{\mathbf{k}}$. A discontinuity of the QP linewidth develops near ω_{LO} for a linear band with a quadratic band top [near the Brillouin zone (BZ) *K* point], while it disappears for a pure linear band (near the BZ *H* point). It is also found that the effective electron-phonon coupling near the *K* point is stronger than near the *H* point by more than 50%. This finding makes possible a consistent understanding of recent angle-resolved photoemission observations near the *K* point.

DOI: 10.1103/PhysRevLett.100.216801 PACS numbers: 81.05.Uw, 79.60.−i, 71.38.−k, 71.20.−b

Graphite is a quasi-two-dimensional material made of hexagonal atomic carbon layers that are weakly coupled to each other. It is an important seed system for many technologically attractive carbon-based materials such as carbon nanotubes and fullerenes [1]. Recently, the observation of stable spontaneous magnetic ordering in hydrogenated graphite has opened up a new possibility for applications in the field of spin electronics [2]. Graphite or layered graphene also attracts great attention because of new fundamental physics such as massless Dirac fermions and quasiparticles (QPs) dynamics in those systems [3]. These have brought new insights and increased interest in the electronic structures of graphite. The electronic structure has been widely studied by angle-resolved photoemission spectroscopy (ARPES) [4–9].

There has been a long-standing debate as to whether or not QPs in a two-dimensional system act as a Fermi liquid. In this regard, there has been much discussion on the normal state QPs in high T_C cuprates, but in that case, the simple QP picture is smashed because of electron correlation, pseudogap, magnetic fluctuation, and so on [10]. In contrast, graphite is a quasi-two-dimensional semimetal or zero-gap semiconductor that provides a simpler test ground for the low-dimensional QP dynamics. A key quantity characterizing the low-energy dynamics is the QP scattering rate, i.e., the inverse of the QP lifetime. The QP scattering rate has been studied both experimentally and theoretically. Theoretically, it is calculated from the imaginary part of the electron self-energy [11,12]. Experimentally, it has usually been measured using time-resolved photoemission spectroscopy (TRPES) [13,14] instead of ARPES, mainly because of the problem of sample quality.

Recently, however, Sugawara *et al.* [8] and Leem *et al.* [9] extracted the QP scattering rate near the Brillouin zone (BZ) *K* point [see Fig. 1(a)] from the linewidth of the ultrahigh resolution ARPES for a high-quality single-crystal graphite. At the BZ *K* point, only the top of the valence band touches the Fermi level. Both groups found that a coupling with the E_{2g} longitudinal optical (LO) phonon of ω_{LO} ($\approx$200 meV) [15] governs the low-energy QP dynamics near the *K* point. However, their experimental conclusions about the impact of phonons on the low-energy dynamics were strikingly different. Sugawara *et al.* [8] have shown that a sharp QP peak in the vicinity of the Fermi level becomes rapidly broadened near ω_{LO} because of a strong electron-phonon coupling, such that a marked discontinuity of the QP linewidth develops. However, Leem *et al.* [9] have reported that the QP linewidth without any discontinuity reflects the effect of the two-dimensional linear band structure and that the electron-phonon coupling is rather weak.

Phase analysis of the quantum oscillations has shown that the two-dimensional hole carriers of graphite are

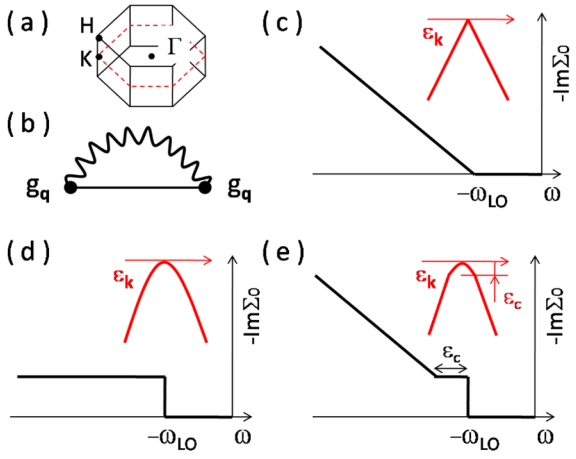

FIG. 1 (color online). (a) Symmetry points in the Brillouin zone. (b) Feynman diagram of the lowest-order self-energy $\Sigma_0(\mathbf{k}, \omega)$. The solid line represents the electron and the wavy line the phonon. (c)–(e) Sketches of $-\mathrm{Im}\Sigma_0(\omega)$ depending on the two-dimensional electronic band dispersions; (c) a linear band, (d) a quadratic band, (e) a linear band with a quadratic band top ($|\varepsilon_{\mathbf{k}}| \propto \mathbf{k}^2$ for $|\varepsilon_{\mathbf{k}}| < \varepsilon_c$).

mixed from the massive quadratic spectrum and the massless Dirac (i.e., linear) spectrum [16]. In fact, an electronic structure calculation of bulk graphite from $k_z = 0$ (the K point) to $k_z = \pi/c$ (c: the unit length along the c-axis, i.e., the H point) shows a change in the band spectra from quadratic to linear [17]. More explicitly, Zhou *et al.* [7] have observed distinguishable band features between the K and H points in ARPES, that is, a quadratic band near the BZ corner K and a linear band near another BZ corner, H. In this Letter, we investigate the low-energy QP dynamics resulting from the electron-phonon coupling in graphite. We find that the low-energy QP dynamics dramatically depends on the underlying electronic band structure of graphite. A discontinuity in the QP linewidth develops near ω_{LO} for a linear band with a quadratic band top ($|\varepsilon_{\mathbf{k}}| \propto \mathbf{k}^2$ for $|\varepsilon_{\mathbf{k}}| < \varepsilon_c$), while it is absent for a pure linear band. The former should correspond to the K point and the latter to the H point. Furthermore, we also find that the effective electron-phonon coupling near the K point is stronger than near the H point by more than 50%.

A nonperturbative approach for the QP spectral function is taken by summing a complete set of diagrams in the narrow band limit corresponding to suppressing the small recoil effect of the valence electron [18]. In the limit, the exact spectral function $J_{\mathbf{k}}(\omega)$ is

$$J_{\mathbf{k}}(\omega) = \frac{1}{2\pi}\int d\tau e^{i(\omega-\varepsilon_{\mathbf{k}})\tau} e^{\{\int d\omega'[\beta_{\mathbf{k}}(\omega')/\omega'^2](e^{i\omega'\tau}-i\omega'\tau-1)\}}, \tag{1}$$

where $\mathbf{k}$ and $\varepsilon_{\mathbf{k}}$ are the two-dimensional electron momentum and band energy, respectively, and $\beta_{\mathbf{k}}(\omega) = (-1/\pi)\mathrm{Im}\Sigma_0(\mathbf{k}, \varepsilon_{\mathbf{k}} - \omega)\Theta(\omega - \varepsilon_{\mathbf{k}})$ with the lowest-order self-energy $\Sigma_0(\mathbf{k}, \omega)$ [$\Theta(\omega)$ is the Heaviside step function]. The greatest merit of this approach is to cover the whole range of electron-phonon (or general boson) coupling strengths [19].

$\Sigma_0(\mathbf{k}, \omega)$ is the lowest-order self-energy at zero temperature resulting from the electron-phonon coupling [see Fig. 1(b)],

$$\Sigma_0(\mathbf{k}, \omega) = \sum_{\mathbf{q}} g_{\mathbf{q}}^2 \frac{1}{\omega + \omega_{\mathrm{LO}} - \varepsilon_{\mathbf{k}+\mathbf{q}} + i0^+}. \tag{2}$$

$g_{\mathbf{q}}$ is the electron-phonon coupling matrix element, and ω_{LO} (≈ 200 meV) is the energy of the E_{2g} LO phonon. The imaginary part of $\Sigma_0(\mathbf{k}, \omega)$ is

$$\mathrm{Im}\,\Sigma_0(\mathbf{k}, \omega) = -\pi\sum_{\mathbf{q}} g_{\mathbf{q}}^2 \delta(\omega + \omega_{\mathrm{LO}} - \varepsilon_{\mathbf{k}+\mathbf{q}}), \tag{3}$$

where $\delta(\omega)$ is the Dirac delta function. If $g_{\mathbf{q}}$ does not have a divergent $\mathbf{q}$-dependency, one can easily examine $-\mathrm{Im}\Sigma_0(\omega)$ from Eq. (3) with $\mathbf{k} = \mathbf{0}$. Putting $g_{\mathbf{q}} \approx g$, it is found that, through the two-dimensional phase-space integration, $-\mathrm{Im}\Sigma_0(\omega)$ depends heavily on the electronic band dispersion of graphite. In Figs. 1(c)–1(e), we sketch the behavior of $-\mathrm{Im}\Sigma_0(\omega)$ for three kinds of typical band dispersions. The discontinuity at $\omega = -\omega_{\mathrm{LO}}$ in Figs. 1(d) and 1(e) will be proportional to g^2. However, the sketches in Figs. 1(c)–1(e) are qualitative and valid only in the limit of weak electron-phonon coupling.

For a quantitative investigation, we adopt the nonperturbative approach for the QP spectral function. The electron-phonon coupling matrix element $g_{\mathbf{q}}$ is taken from monolayer graphene, i.e., $g_{\mathbf{q}}^2 \approx g^2[1 - \cos 2\theta_{\mathbf{q}}]$ in the long wavelength limit [20], where $\theta_{\mathbf{q}}$ is the polar angle of $\mathbf{q}$ with respect to the electron momentum. The present form of $g_{\mathbf{q}}$ with just a smooth $\mathbf{q}$-dependency justifies the qualitative illustration in Fig. 1. In an actual situation, the interlayer coupling splits the p_z-derived π bands into a nonbonding band (touching the Fermi level) and a bonding band (more extensively lowered relative to the Fermi level) at the K point [21]. However, the splitting disappears at the H point. Assuming a weak interband transition, only the nonbonding band closer to the Fermi level will be considered. A calculation of $\beta_{\mathbf{k}}(\omega)$ is then straightforward by assuming a bare band dispersion for a single nonbonding band. The nonperturbative spectral function $J_{\mathbf{k}}(\omega)$ can be evaluated by transforming Eq. (1) to the form of an integral equation [19].

Incorporating a pure linear band such as $\varepsilon_{\mathbf{k}} = -\gamma|\mathbf{k}|$ ($\gamma = 6$ eV Å), we show the low-energy QP dynamics near the BZ H point in Fig. 2. In Fig. 2(a), we plot $\beta_{\mathbf{k}}(\omega)$, which is defined from $\mathrm{Im}\Sigma_0(\mathbf{k}, \omega)$ in a slightly different fashion. $\beta_{\mathbf{k}}(\omega)$ shows that a QP positioned in the vicinity of the Fermi level cannot decay. That is, a case of $E_B = 50$ or 100 meV ($E_B = |\varepsilon_{\mathbf{k}}|$ for a given $\mathbf{k}$, i.e., the bare binding

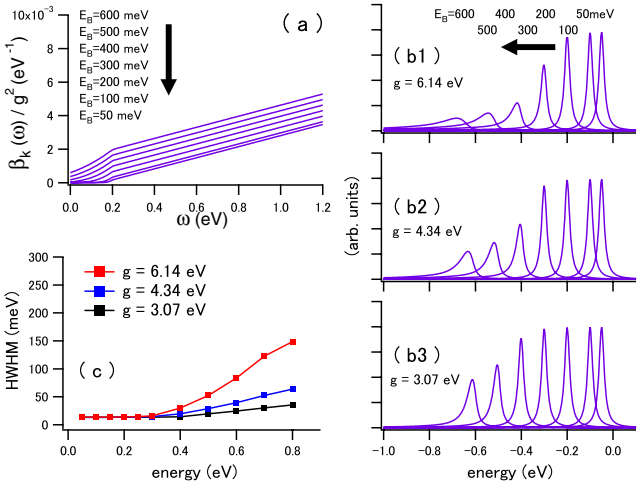

FIG. 2 (color online). Low-energy QP dynamics near the BZ H point. A linear electronic band is used; $\varepsilon_{\mathbf{k}} = -\gamma|\mathbf{k}|$ ($\gamma = 6$ eV Å). (a) $\beta_{\mathbf{k}}(\omega)/g^2$ with respect to for binding energies. A value of $\mathbf{k}$ is given through the bare binding energy E_B ($= |\varepsilon_{\mathbf{k}}|$). (b1)–(b3) Electron spectral functions with respect to binding energies for given values of g. Convolution with a 10 meV Lorentzian is applied to each spectral function. (c) Half-width at half-maximum (HWHM) with respect to binding energies for given values of g.

energy) gives a well-defined sharp (convolution limited) Lorentzian in Figs. 2(b) (1)–(3). On the other hand, a QP positioned far away from the Fermi level can decay, which gives the asymmetrically broadened spectral function on the high-binding-energy side in Figs. 2(b) (1)–(3). The asymmetry can be understood from a phase-space consideration of the continuous energy loss. The half-width at half-maximum (HWHM), i.e., the linewidth, of the broadened spectral function gives the QP scattering rate, $1/\tau$, which is the inverse of the QP lifetime, τ. In Fig. 2(c), it is shown that the QP scattering rate starts to be nonzero near ω_{LO} and continuously increases without any kink or discontinuity. When g is small (weak coupling), the increase in the scattering rate is linear over ω_{LO}. This is consistent with the lowest-order sketch in Fig. 1(c). However, when g is large (strong coupling), the scattering rate deviates from linear behavior.

In contrast, the low-energy dynamics near the BZ K point are examined in Fig. 3 by incorporating a linear band with a quadratic band top, as in the inset of Fig. 1(e). In this case, the electronic band dispersion is assumed as follows: for $|\varepsilon_{\mathbf{k}}| < \varepsilon_c$, $\varepsilon_{\mathbf{k}} = -\mathbf{k}^2/2m^*$, and otherwise $\varepsilon_{\mathbf{k}} = -\gamma|\mathbf{k}| + \eta$ together with $\varepsilon_c = 112$ meV [22] and $|\mathbf{k}_c| = 0.057$ Å^{-1}. m^* and η are constants determined from the band connection. Unlike the H point [Fig. 2(a)], we note abrupt jumps of $\beta_{\mathbf{k}}(\omega)$ near $\omega_{\mathrm{LO}} - E_B$. This leads to a sudden broadness in the spectral function at $E_B \approx \omega_{\mathrm{LO}}$ or higher binding energy, which is shown in Figs. 3(b) (1)–(3). In Fig. 3(c), we display the behavior of the HWHM with respect to binding energies for given values of g. Further, we point out discontinuous jumps in

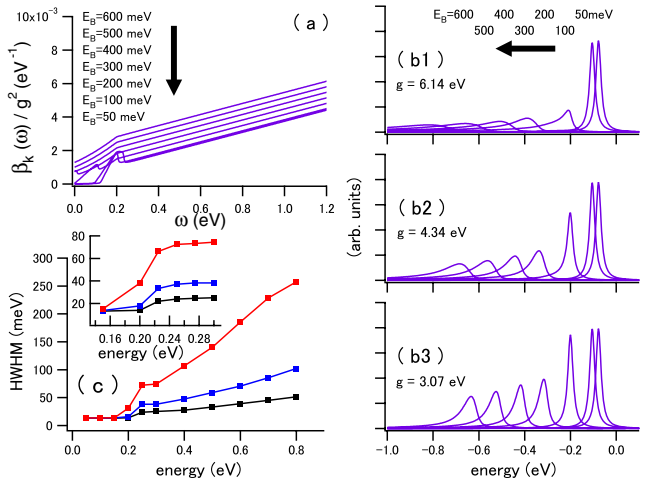

FIG. 3 (color online). Low-energy QP dynamics near the BZ K point. A linear electronic band with a quadratic band top is used; for $|\varepsilon_{\mathbf{k}}| < \varepsilon_c$, $\varepsilon_{\mathbf{k}} = -\mathbf{k}^2/2m^*$, and otherwise, $\varepsilon_{\mathbf{k}} = -\gamma|\mathbf{k}| + \eta$ with $\varepsilon_c = 112$ meV at $|\mathbf{k}_c| = 0.057$ Å^{-1}. In the inset of (c), more detailed behaviors of HWHM are given in a narrow region around 0.2 eV. The description for each figure panel is the same as in Fig. 2. The parametric legends omitted in (c) are also the same as in Fig. 2(c).

the QP scattering rate near ω_{LO}, which is dramatically contrasted with the results at the H point [Fig. 2(c)]. These discontinuities are robust for all values of g. We also point out that the absolute value of the scattering rate at the K point is much larger than at the H point for the same parametric condition of the electron-phonon coupling.

For a reliable estimation of the effective electron-phonon coupling strength at both BZ points, we need the electron-phonon mass enhancement factor λ, defined by $\lambda = -\partial \mathrm{Re}\Sigma(\omega)/\partial\omega|_{\omega=0}$. The infinite-order spectral function in our nonperturbative treatment does not guarantee achieving the infinite-order self-energy, i.e., $\Sigma(\omega)$. Symmetrizing the behavior of the HWHM in Figs. 2(c) and 3(c), the real parts of the self-energy are calculated through the Kramers-Kronig relation. Figure 4 shows the behavior of $\mathrm{Re}\Sigma(\omega)$ for given values of g at the BZ points. In Table I, the mass enhancement factors at the H and K points for given values of g are listed. At least for the given values of g, it is found that the effective electron-phonon coupling at the K point is stronger than at the H point by more than 50%. This is consistent with Zhou *et al.* [7], where the ARPES signal from the K point is found to decay much faster than that from the H point in the high-binding-energy region ($E_B > \omega_{\mathrm{LO}}$) even if quantified values of λ are not provided. $\lambda \gg \lambda_0$ means that the present nonperturbative theory is taking into account the nontrivial higher order coupling effect beyond the lowest-order effect.

The low-energy QP dynamics at the two BZ points found in our analysis provide important physical meaning for recent controversial ARPES experiments. Sugawara *et al.* [8] have reported a well-defined sharp QP peak near the Fermi level and anomalous QP lifetime with a marked discontinuity around 200 meV near the K point, which they have attributed to the strong electron-phonon coupling. They have also estimated $\lambda = 1.0 \pm 0.1$ (two-dimensional model). On the other hand, Leem *et al.* [9] have reported completely different observations through the same ARPES observation for the same sample [23]. They have observed the QP linewidth following the effect of linear density of states without any kink or discontinuity. In addition, they have estimated that λ will be at most 0.2 as the upper bound value.

As concluding remarks, we make comments on the physical implications of two conflicting ARPES observations based on our theoretical results. First, in order to

TABLE I. The electron-phonon mass enhancement factor λ at the BZ H and K points. λ_0 is the lowest-order mass enhancement factor, i.e., $\lambda_0 = -\partial \mathrm{Re}\Sigma_0(\omega)/\partial\omega|_{\omega=0}$.

g (eV)	λ (λ_0) (H point)	λ (λ_0) (K point)
6.14	0.48 (0.08)	0.78 (0.148)
4.34	0.21 (0.04)	0.31 (0.074)
3.07	0.10 (0.02)	0.15 (0.037)

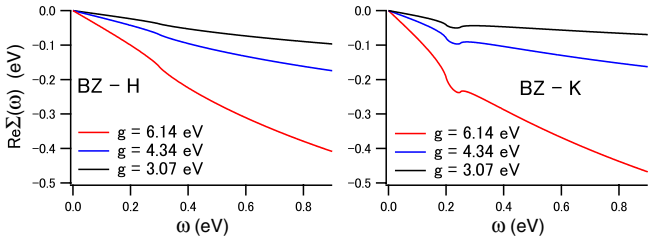

FIG. 4 (color online). Real parts of the self-energy $\mathrm{Re}\Sigma(\omega)$ near the BZ H and K points for given values of g.

match quantitatively the discontinuity observed in Sugawara *et al.*, the electron-phonon coupling as strong as $\lambda \approx 1$ is required. However, according to our analysis, the strong coupling to give $\lambda \approx 1$ will result in the QP linewidth increasing much faster than their observation in the high-binding-energy region, i.e., $E_B > \omega_{\mathrm{LO}}$ [see Fig. 3(c)]. This is a nontrivial disagreement with our results. Second, being different from the first, Leem *et al.*'s results could be taken as the weak coupling case at the K-point, for instance, $g = 3.07$ eV ($\lambda = 0.15$) in Fig. 3(c). Even if any kink or discontinuity is not observed in their results, we note that a small jump near ω_{LO} might be smeared in the photoemission spectra by the extra broadening not explicitly considered in our study. One of the important sources would be from the finite escape depth of the photoelectron, i.e., the broadening due to the k_z dispersion [24]. Roughly, this leads to an additional broadening of $(\Delta k_z)^2/2m^*_{K-H}$ to our present calculation of the spectral function [25]. When taking the maximum possible broadening ($\approx$30 meV), the discontinuity in the QP linewidth would be smeared if its size is smaller than about 30 meV. With this criterion, $\lambda \sim 0.2$ (of Leem *et al.*'s) would be rather small or marginal to give the apparent discontinuity. It is then found that Leem *et al.*'s results do not contradict our results. Accordingly, it becomes clear that our theoretical consideration is consistent with the weak coupling case ($\lambda \sim 0.2$ would be close to the upper bound).

To summarize, we have found that there are sharp contrasts between the BZ K and H points in the low-energy QP dynamics of graphite, which are governed by a coupling with the E_{2g} LO phonon of $\omega_{\mathrm{LO}} \approx 200$ meV. The origin is the difference in the electronic band dispersion between the BZ K and H points. A discontinuous jump in the QP linewidth evolves near ω_{LO} for a linear band with a quadratic band top (near the BZ K point), while it is removed for a pure linear band (near the BZ H point). The effective electron-phonon coupling near the K point is stronger than near the H point by more than 50%. This finding makes possible a consistent understanding of recent controversial ARPES experiments.

We thank Changyoung Kim for constructive discussions on the latest ARPES observations. We also thank Rainer Friedlein for bringing our attention to Ref. [8]. This work was supported by Special Coordination Funds for Promoting Science and Technology from MEXT, Japan.

[1] M. S. Dresselhaus *et al.*, *Science of Fullerene and Carbon Nanotubes* (Academic Press, San Diego, 1996).
[2] P. Esquinazi *et al.*, Phys. Rev. Lett. **91**, 227201 (2003).
[3] A. Bostwick *et al.*, Nature Phys. **3**, 36 (2007).
[4] V. N. Strocov *et al.*, Phys. Rev. B **64**, 075105 (2001).
[5] T. Kihlgren *et al.*, Phys. Rev. B **66**, 235422 (2002).
[6] K. Sugawara *et al.*, Phys. Rev. B **73**, 045124 (2006).
[7] S. Y. Zhou *et al.*, Nature Phys. **2**, 595 (2006).
[8] K. Sugawara *et al.*, Phys. Rev. Lett. **98**, 036801 (2007).
[9] C. S. Leem *et al.*, Phys. Rev. Lett. **100**, 016802 (2008).
[10] A. Damascelli *et al.*, Rev. Mod. Phys. **75**, 473 (2003).
[11] J. Gonzales *et al.*, Phys. Rev. Lett. **77**, 3589 (1996).
[12] C. D. Spataru *et al.*, Phys. Rev. Lett. **87**, 246405 (2001).
[13] S. Xu *et al.*, Phys. Rev. Lett. **76**, 483 (1996).
[14] G. Moos *et al.*, Phys. Rev. Lett. **87**, 267402 (2001).
[15] L. Vitali *et al.*, Phys. Rev. B **69**, 121414(R) (2004).
[16] I. A. Luk'yanchuk and Y. Kopelevich, Phys. Rev. Lett. **93**, 166402 (2004).
[17] D. Graf *et al.*, Nano Lett. **7**, 238 (2007).
[18] L. Hedin, Phys. Scr. **21**, 477 (1980).
[19] J. D. Lee and A. Fujimori, Phys. Rev. Lett. **87**, 167008 (2001).
[20] T. Ando, J. Phys. Soc. Jpn. **75**, 124701 (2006).
[21] R. C. Tatar and S. Rabii, Phys. Rev. B **25**, 4126 (1982).
[22] $\varepsilon_c = 112$ meV may belong to a smaller side. ε_c could be estimated to be 200–400 meV from recent ARPES observations [7–9].
[23] In fact, Sugawara *et al* [8] used a kish graphite and Leem *et al* [9] a natural graphite single crystal. However, the difference is not considered crucial.
[24] This broadening is, of course, relevant only to the photoemission experiment.
[25] Δk_z ($\approx 1/l$) is the uncertainty in the value of k_z determined from the escape depth $l \approx 7$ Å [9], and m^*_{K-H} is the effective electron mass determining the electronic structure along the $K - H$ direction. m^*_{K-H} is roughly taken from $(\pi/c)^2/2m^*_{K-H} \lesssim 0.35$ eV, i.e., the half of the maximum π-band splitting (see the schematic in Fig. 2(c) of Ref. [9]). c is 6.7 Å, the lattice constant along the c-axis. Finally, the broadening results $(\Delta k_z)^2/2m^*_{K-H} \lesssim 30$ meV.